

INTERFEROMETRIC SIDE-SCAN SONAR A TOPOGRAPHIC SEA-FLOOR MAPPING SYSTEM

by Dr. Dieter KOLOUCH(*)

ABSTRACT

The knowledge of bottom topography of our oceans is one of the requirements for engineering and marine geology. Particularly in shallow coastal areas, however, topography is frequently changed by storms and tidal currents. Repeated surveys at short intervals are necessary for up-to-date information. The employment of echo-sounders, which can take one depth profile at a time, is time consuming and means great expense for this work. This paper presents a new system called Interferometric Side-Scan Sonar (ISSS), that records images with fringe patterns which are geometrically related to several depth profiles. The evaluation of these data is done by digital image processing methods with respect to a geometrical model for the recording situation. Necessary additional data for orientation such as rotation and positioning of the sensor are taken into account.

1. INTRODUCTION

Side-scan sonar is nowadays an operational underwater system for sea-floor mapping. The system, containing transducers for sound propagation, is towed by a ship and transmits acoustic pulses orthogonal to the towing direction. The emitted acoustic field is vertically wide open and horizontally narrow, which has the effect that each single pulse only "sounds" a small sea-floor strip. The reflections from the sea-bottom (echoes) are received by the same transducers and recorded in an image line, wherein the position of an image point corresponds to the target range (determined by signal running time) and the point density to the

(*) Universität Hannover, Sonderschungsbereich 149, Nienburger Strasse 1, D 3000 Hannover 1, Fed. Rep. of Germany.

echo intensity. By towing the sensor and repeatedly transmitting and receiving the sound, an image is built up line by line.

Side-scan sonar images (see fig. 1) are mainly used for the detection of natural and man-made bottom features such as rocks, sand ripples, boulders, shipwrecks, pipe-lines, sea-bed engineering activities, etc. They are taken for control purposes, for change detection and for geologic interpretations. For the overview of greater areas, two or more image strips can be combined into a mosaic. This requires, for acceptable interpretation, a rough geometric correction of the single strips before mosaic production. Standard correction procedures are the conversion from the obtained slant-range image to ground-range presentation for uniform scale in transmitting direction and the adaptation of the scale in towing direction. This can be done optically, with some difficulties. A much better way is the correction by digital methods if data are recorded on tape (KOLOUCH, 1983). Little is known of activities involving application of side-scan sonar to geodetic survey to obtain depth information from these images. Tests made by MITTLEMAN and MALLOY and by CLERICI (1977) dealt with photogrammetric stereoscopic methods from overlapping image strips. These tests were only partly successful. The difficulties for stereoscopic processing mainly stem from the lack of point correlation in both images, due to image quality and the fact that standard side-scan sonar images normally contain insufficient "acoustically" prominent topographic details of the sea bottom. The second reason for the preclusion of stereoscopic viewing is the relative geometrical distortion of each single image because of sensor movement. These two reasons restrict stereoscopic methods to point-wise techniques.

More successful for broad area depth determination from side-scan sonar images is the application of interferometric methods. The foundation of this technique is the mixing of coherent signals travelling along different paths to a surface target, then back to the receiver. This creates fringe patterns in the image, which are extremely sensitive to depth changes. In this field previous studies have

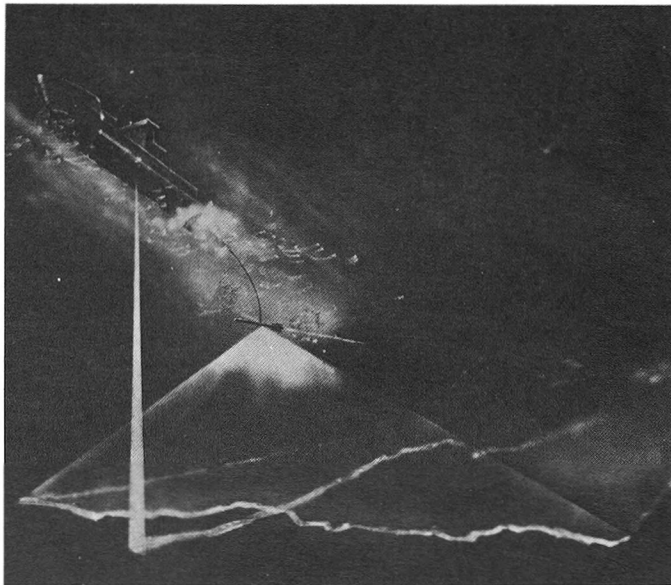


FIG. 1. — Side-scan sonar system (EG&G).

been done by CHESTERMAN (CHESTERMAN *et al.*, 1967) and HEATON (HEATON and HASLETT, 1971) with patterns caused by surface reflection (Lloyd mirror effect) and by STUBBS (STUBBS *et al.*, 1974) using a pressure reflector. Newer developments have been done by PARKER VERBOOM (1982) and KLEPSVIK (1983) and last but not least by the author (KOLOUCH, 1983 *a*). In a "Special Research Project" at Hannover University, called "Vermessungs- und Fernerkundungsverfahren an Küsten und Meeren", an interferometric hardware system was developed. The evaluation of the image data recorded by this equipment is done by digital image processing software. To get absolute three-dimensional co-ordinates from the image, positioning and angular movements of the platform are taken into account.

2. FUNDAMENTALS OF INTERFEROMETRIC FRINGE PATTERN

2.1. Lloyd mirror effect

The natural Lloyd mirror effect appears in standard side-scan sonar images only under special weather conditions. The sea-surface must be considerably calm and work as a mirror. The fan-shaped sound beam then reaches the sea-bed on two paths, directly and by a reflected path due to sea-surface reflection.

Such signals from the same transmitters are coherent and can interfere. If the path difference is an odd number of half wave-length (because of phase-change of 180° at surface reflection) the resulting signal is reinforced, otherwise at differences of even numbers it is cancelled. Due to different ranges and view-angles many reinforcements and extinctions are recorded and repeated transmissions give a series of fringe patterns in the sound image (Fig. 2).

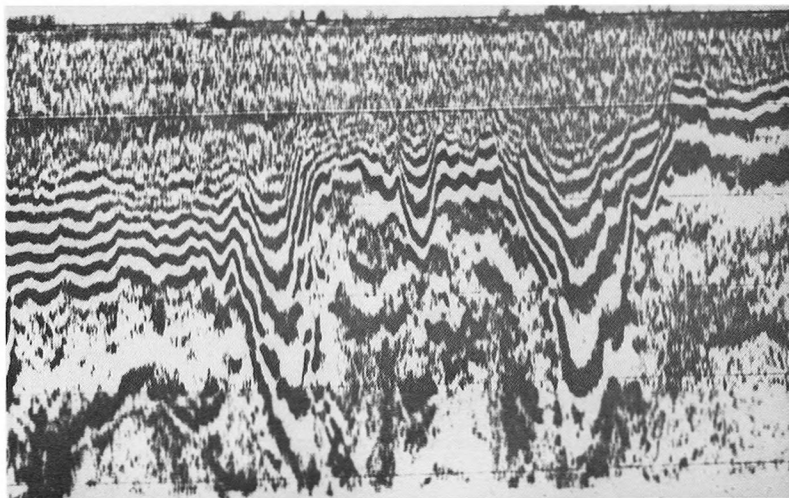


FIG. 2. — Lloyd mirror in standard sonar image (from BELDERSON *et al.*, 1972).

The corresponding geometric situation of Lloyd mirror is shown in a simplified manner in Figure 3. Confined to signal reinforcement — later called interference — this geometry leads to expressions for the determination of water depth and horizontal distance for an interference point P_n . Because of the physical situation, range and recording direction can be fixed.

The path difference of the two signals can be expressed as

$$\overline{O'P} - R_n = (2n - 1) \cdot \frac{\lambda}{2} = (n - \frac{1}{2}) \cdot \lambda \quad (1)$$

Referring to Figure 3 are

$$\overline{O'P} = ((Z_n + d)^2 + Y_n^2)^{1/2} \quad (2)$$

and

$$Y_n^2 = R_n^2 - (Z_n - d)^2 \quad (3)$$

The combination of (1), (2) and (3) leads to

$$Z_n = \frac{(2n - 1) \cdot \lambda \cdot R_n}{2d} + \frac{(n - \frac{1}{2})^2 \cdot \lambda^2}{4d} \quad (4)$$

$$Y_n = (R_n^2 - (Z_n - d)^2)^{1/2} \quad (5)$$

where n = number of fringe areas

R_n = range of P_n (can be taken from image referring to scale)

λ = wavelength used

d = towing depth

Z_n = water depth of P_n

Y_n = horizontal distance of P_n

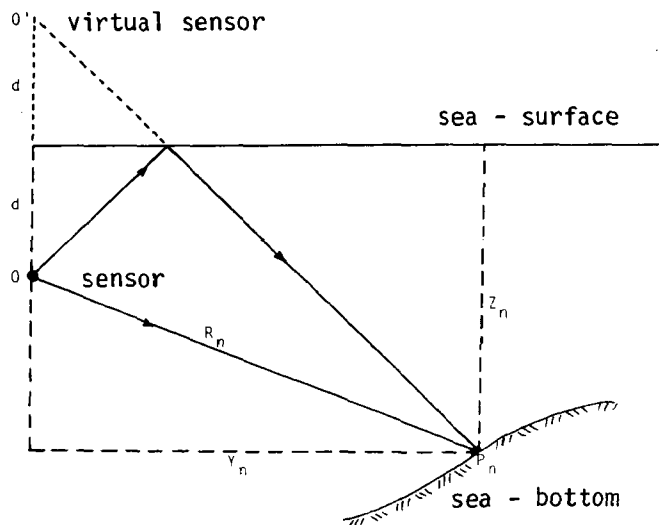


FIG. 3. — The geometry of Lloyd mirror.

The equations (4) and (5) are the fundamental relations for the determination of discrete three-dimensional co-ordinates from a two-dimensional image if fringe order n and towing depth d are known. The missing co-ordinate X_n is exclusively given by the sensor position due to ship's speed and recording time.

2.2. Synthetic processing of interference fringes

The natural appearance of Lloyd mirror fringes is limited because of wind and weather conditions. For a convenient use of this effect for topographic mapping it has to be processed synthetically. Preserving the hydrodynamic properties of a towing system, it is necessary to use two transducers which work exactly synchronously and are transmitting to the same side and in the same plane. The interference geometry then is simplified because of loss of surface reflection. This situation is shown in Figure 4 (KOLOUCH, 1980).

The water depth is now calculated with the sensor's centre as zero point. There is no longer a phase change at reflection and therefore path difference now has to be an integer number of wavelength used. The towing depth is replaced by

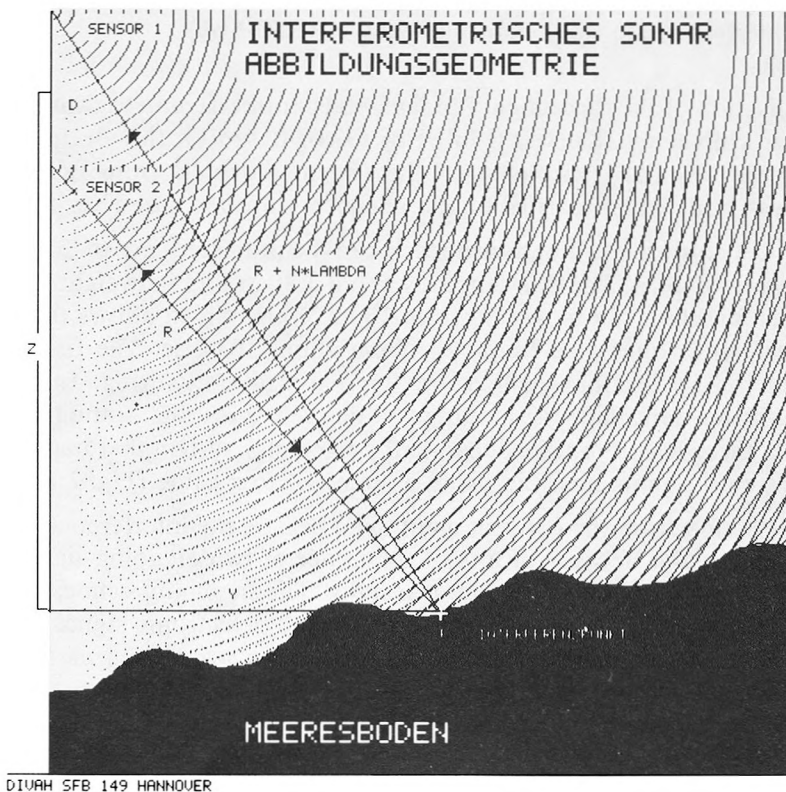


FIG. 4. — Interference pattern processing using two transducers.

half of sensor's distance D . With regard to this situation the equations (4) and (5) change to

$$Z_n = \frac{R_n \cdot n \cdot \lambda}{D} + \frac{n^2 \cdot \lambda^2}{2D} \quad (6)$$

$$Y_n = (R_n^2 - (Z_n - \frac{D}{2})^2)^{1/2} \quad (7)$$

3. THE INTERFEROMETRIC SIDE-SCAN SONAR EQUIPMENT

The equations (6) and (7) are valid only for the case of an absolute vertical baseline D between the two transducers. This is not given because of the dynamic towing situation. Mainly, rolling in ω changes the effective direction of the co-ordinate reference plane and leads to a wrong determination of the water depth Z_n , if this parameter is not recorded and corrected. Pitch (Φ) and yaw (κ) have more influence on X_n and Y_n co-ordinates and falsify water depth only little. Nevertheless, synchronous recording of all angular parameters is necessary for further evaluations.

3.1. The interferometric side-scan sonar sensor (ISSS-Fish)

Realisation of the theoretical fundamentals of interferometric sonar was made at Hanover University (KOLOUCH in SFB, 1979). Based on the electronic components and the original transducers of the system Mark 1B from EG & G, a new tow-fish was built which carries both transducers on one side (Fig. 5).

The depression of the transducers can be adjusted up to 35° down for different water depths. The fish length is about 1.30 m and its weight is 72 kg. The transducers' baseline can be varied from 10 to 25 cm, which allows the processing of 17 interference lines at a frequency from about 105 kHz. The fish is made of aluminium hollow sections, which are flooded while surveying. Inside the fish (Fig. 6) a water-tight tube is mounted which contains the standard electronic elements, a three-axis rate transducer, and a telemetry system that makes transmission of the rate signals possible using a standard tow cable (Fig. 7 and Fig. 8).

In deviation from the concept mentioned before, the interference patterns are produced indirectly. Because of loss of coherence of two outgoing signals from the two transducers, only the lower one transmits. The incoming echoes are received by both, and the interference signal is processed by electronic signal mixing. This procedure has the added advantage of synchronous processing of standard and interferometric sonar images, which are in this system recorded on the original port and starboard channels.

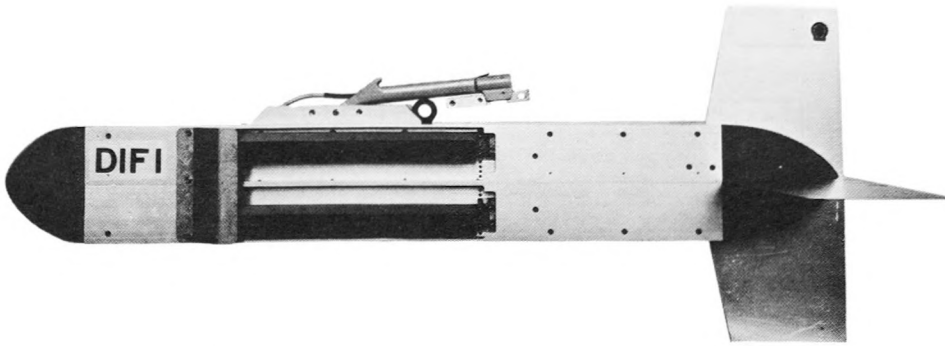


FIG. 5. — Interferometric side-scan sonar fish (closed).

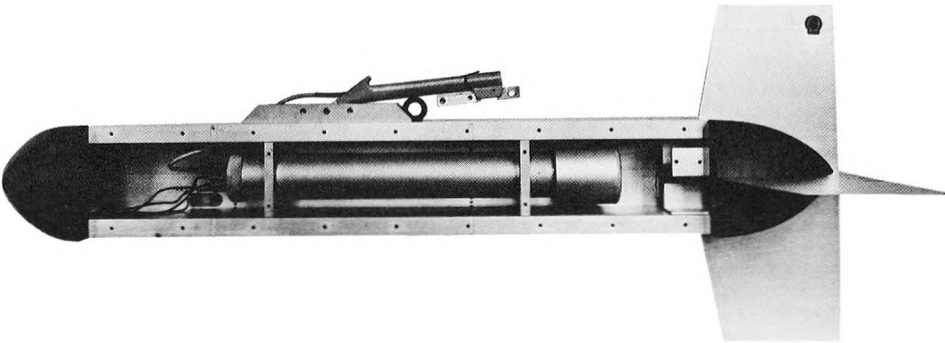


FIG. 6. — Interferometric side-scan sonar fish (open).

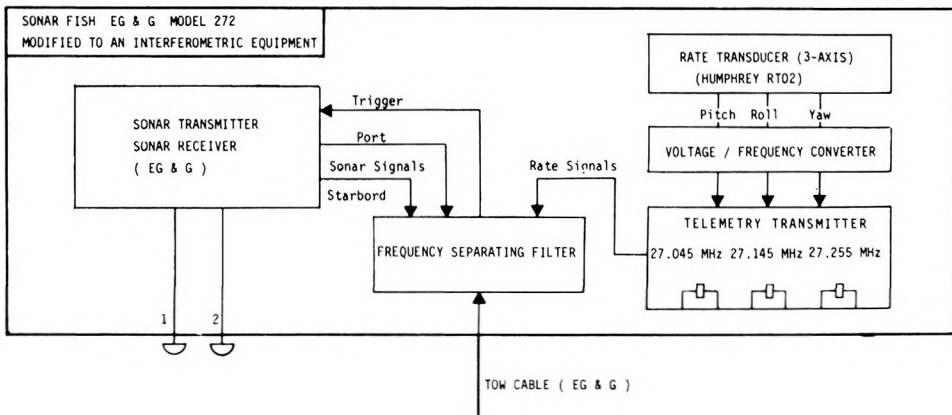


FIG. 7. — Electronic equipment in the ISSS-fish.

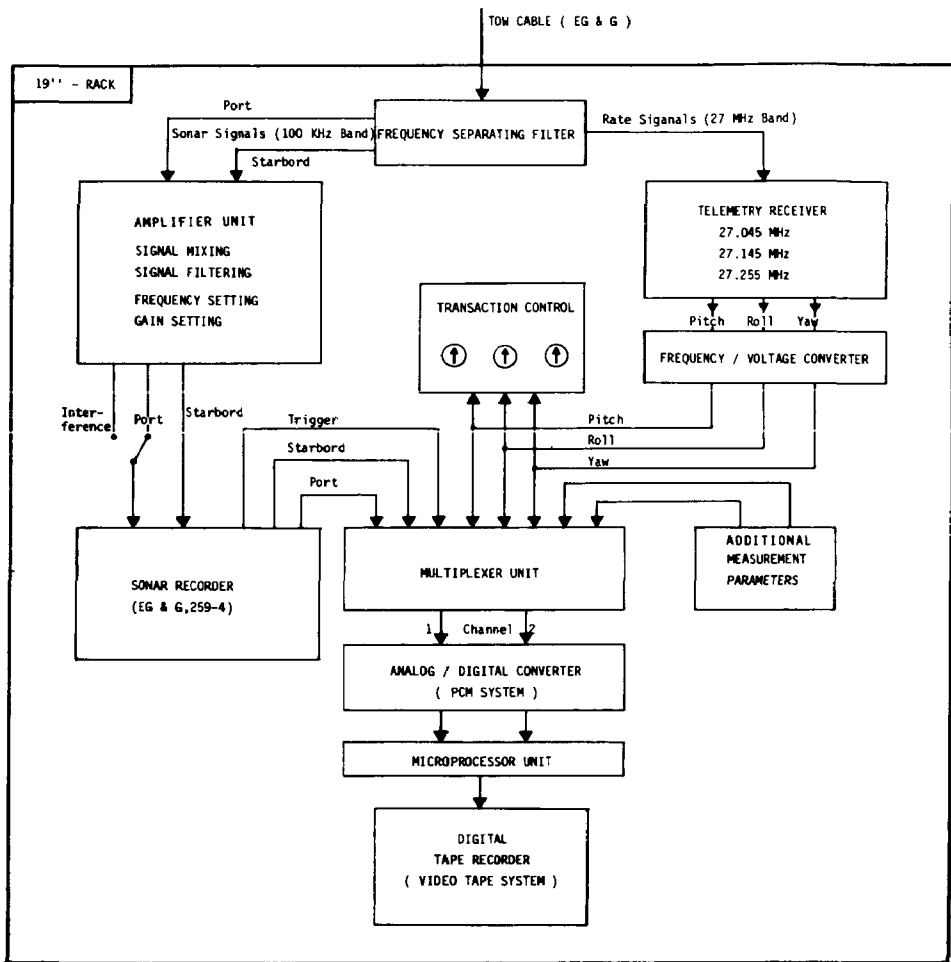


FIG. 8. — System for data pre-processing and recording.

3.2. A special system for data pre-processing and recording

Signal processing and recording is still controlled by a standard recorder of the EG & G system. Between fish and recorder special data processing equipment is installed to house the electronic signal mixing unit, which includes a changeable low-pass filter and a frequency control unit. This system also contains the electronics for separation of the rate-transducer signals and the two image data strings. All information is stored on PCM-controlled videotape, organized as follows : one channel on the tape starts with the rate signals, followed by the image data of an interferometric image line, while the other channel gets the standard sonar signal with the trigger pulse at the beginning. Trigger and rate signals are recorded with negative sign and are later used as indicators for line start at analog/digital conversion. The electronic parts are installed in a transportable cabinet, which makes employment on different vessels possible.

4. THE DATA PROCESSING SOFTWARE SYSTEM

The hardware system presented earlier is a prototype for interferometric sonar imaging with the aim of processing these data for the determination of three-dimensional space co-ordinates from the sea-bottom. The system works up to a water depth of about 60 m and to ranges up to 150 m. Figure 9 shows a part of a track recorded near Hoek van Holland in co-operation with the North Sea Directorate of Rijkswaterstaat in the Netherlands.

The concept has always been to process the obtained data off-line with digital methods. This is done by special image processing software, which is part of an extensive modular software system at Hanover University called MOBI (German : Modulares Off-line Bildverarbeitungssystem), that is made for the evaluation of remote sensing data (KOLOUCH *et al.*, 1981). The videotape recorded sonar data are first of all digitized by using an A/D-converter and a double buffer interface at a DEC VAX 11/750 computer system. The images are stored on CCT (computer compatible tape) for further evaluation. A pre-requisite for this is the development of a geometrical and mathematical model.

4.1. A geometrical-mathematical model for data evaluation

Side-scan sonar is a dynamic imaging system and therefore the definition of mathematical connections between image co-ordinates and space co-ordinates depends on the recording time. In this case each image line is recorded with its own geometric situation. This will be marked in the following expressions by the index j .

According to figure 10 four orthogonal co-ordinate systems will completely define geometry of imaging at time t_j .

$X_j^i (X_j^i, Y_j^i, Z_j^i)$	“dynamic” sensor system, rotating around its origin due to time
$U_j^i (U_j^i, V_j^i, W_j^i)$	“static” sensor system, defined with horizontal plane U, V in the same origin
$U_j (U_j, V_j, W_j)$	ship’s co-ordinate system, parallel to the U_j^i system with the U axis in the ship’s course direction, origin in ship’s centre
$R (R, H, Z)$	reference co-ordinate system.

The connections between these systems can be found easily : X_j^i can be transformed to U_j^i (both have the same origin) using a rotational matrix A_j , which contains functions of pitch, roll and yaw. Co-ordinates fixed in U_j^i are transformed to U_j with respect to translational parameters α_j , β_j and d , using functions of them in the matrix B_j . Finally, a simple co-ordinate transformation from U_j to R is necessary with respect to the measured positioning data of the ship. This is done in sequences between two positioning points P_{oi} and P_{oi+1} by the valid matrix D_i .

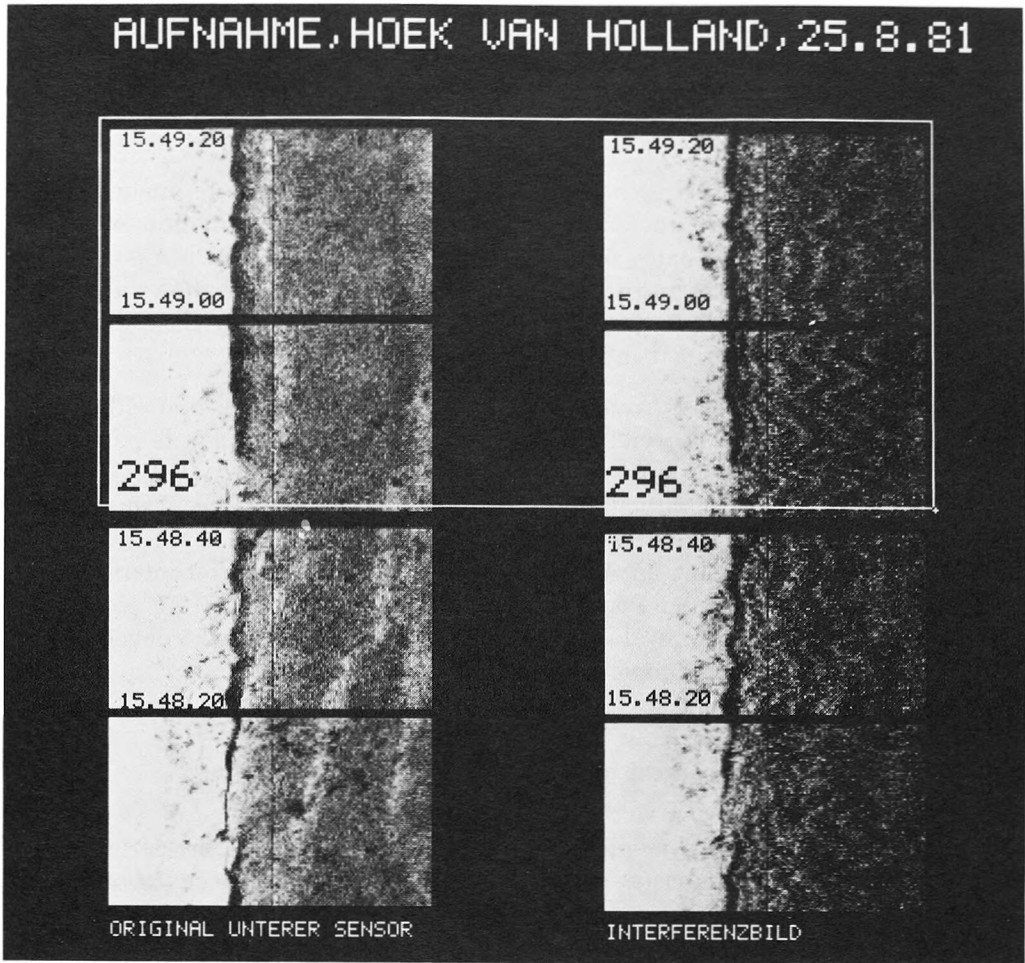


FIG. 9. — Synchronously recorded interferometric and standard sonar images.

In summary, the equations for the determination of space co-ordinates for discrete interference points are :

$$\begin{bmatrix} R_{p_i} \\ H_{p_i} \\ Z_{p_i} \end{bmatrix} = \begin{bmatrix} R_{o_i} \\ H_{o_i} \\ 0 \end{bmatrix} + \mathbf{D}_i \cdot \begin{bmatrix} \Delta U_j \\ 0 \\ 0 \end{bmatrix} + \mathbf{A}_j \cdot \begin{bmatrix} 0 \\ Y'_{p_{ij}} \\ Z'_{p_{ij}} \end{bmatrix} + \mathbf{d} \cdot \mathbf{B}_j \quad (8)$$

For these expressions two important points have to be mentioned : the ΔU_j co-ordinate depends exclusively on ship's speed and is linear, determined from the recording sequence of the image line, using the time between two positionings. The connection to the image is only given if these positions are marked in the image

(by event mark switch). The co-ordinates input in the equations (8) are Y'_{p_i} and Z'_{p_i} , which are determined from the image co-ordinates by using (6) and (7). That means the processing of space co-ordinates in the co-ordinate system X'_{p_i} from all the image is done before determination of (8). Using digital image pre-processing routines this can be done automatically, and by this all the evaluation process is automated.

4.2. Determination of interference pattern image co-ordinates

Digitized images are organized in raster co-ordinates. Each image point is fixed by row and column and has an allocated density in integer values between 0 and 255 (8-bit conversion). The automatic determination of the image co-ordinates for the fringe pattern is, in each individual row which contains the original data, really difficult. Figure 11 shows the reason. While the human eye can detect the pattern by integrating the whole image information; it is not possible for a single row, as the densitometric profile shows. Six maxima values should be found. These difficulties stem from strong image noise caused by the different electronic elements for signal processing. Noise has to be removed for further operations.

Tests with simple digital filters like moving average or median filtering did not give the desired results (KOLOUCH in SFB, 1982). To find a better working filter function, the image was analysed by Fourier transformation (CASTLEMAN, 1979). This could be done one-dimensionally, because the image contains parts where no sound reflection takes place. In this area no image information is received, while the electronic elements are already working, so only noise is present.

Figure 12a) shows the power spectrum. There is no longer loss of intensity at frequencies greater than $0.2 f_N$ ($f_N = \text{Nyquist frequency}$). In these frequency areas more noise than signal is present. As a result of this analysis a low-pass filter function was designed (Fig. 12b), which works in the space domain. Filtering in the frequency domain was tested too, but did not give essentially better results.

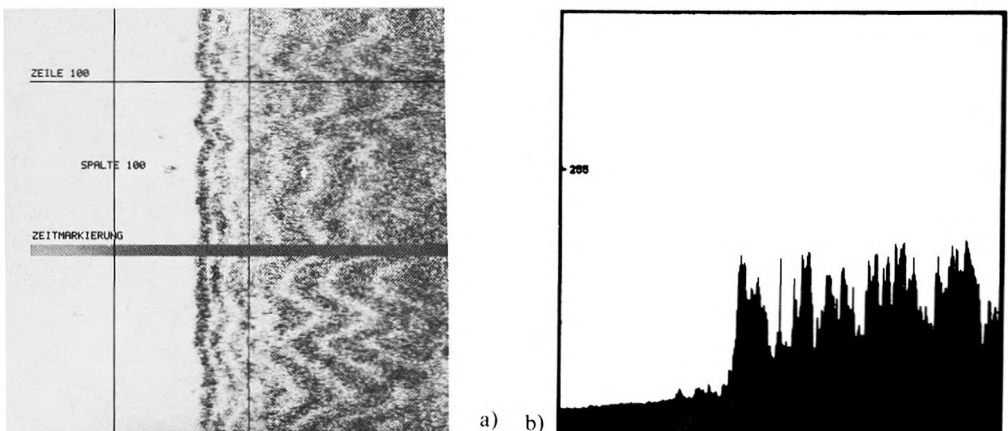


FIG. 11. — Interferometric sonar image with densitometric row profile.

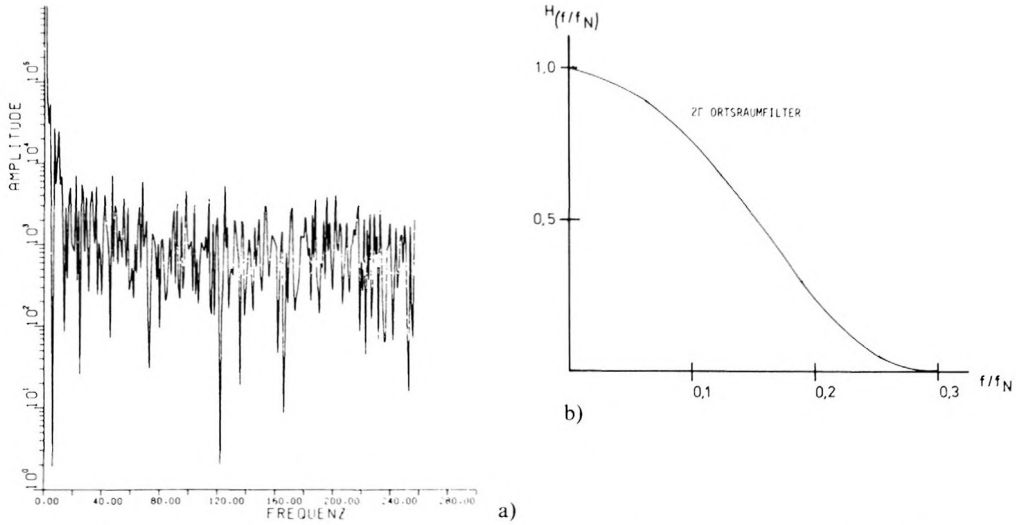


FIG. 12. — a) One-dimensional Fourier transform, and b) designed filter function.

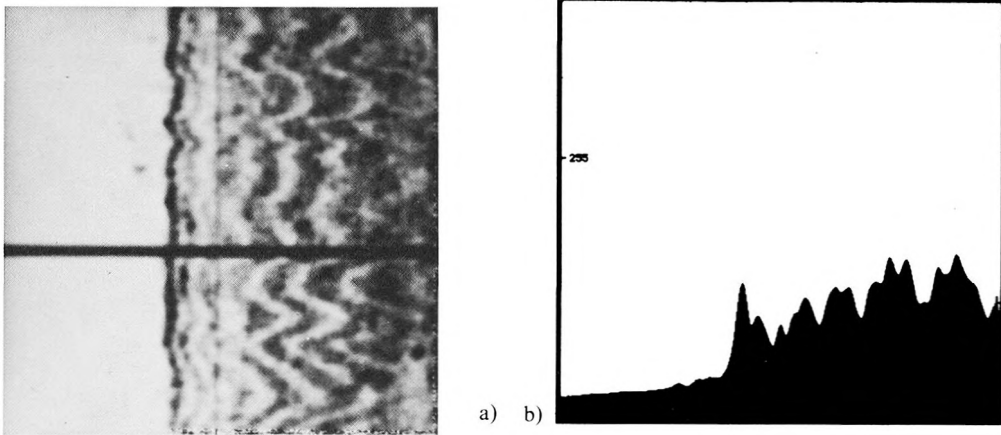


FIG. 13. — a) Filtered ISSS-image, with b) densitometric row profile.

The filter result is seen in Figure 13a), again shown with a densitometric profile of the same row. The image became blurred, but the profile demonstrates that an automatic pattern detection now is possible, in following simple procedures (EHLERS and KOLOUCH, 1982).

5. CONCLUSIONS

The developed hardware equipment for synchronous interferometric and standard sonar imaging allows, in combination with the introduced software package, the determination of discrete three-dimensional co-ordinates from two-

dimensional image co-ordinates. These data can be used for further processing with different aims. This can be the interpolation of a Digital Terrain Model (DTM) with following automatic depth-line plotting. Figure 14 shows an example, which was processed from only one short interferometric side-scan sonar record.

On the other hand, the data obtained can be used for the rectification of the standard sonar image. These modules, made for the rectification of air-borne remote sensing data, are installed in MOBI (DENNERT-MÖLLER *et al.*, 1982). An overlay of both in combination with digital mosaicking leads to an orthophotomap from the sea-bottom containing topographic information. The hardware system was first tested in late 1981 in the North Sea in front of Hoek van Holland. It was towed over a test area where depth data was well known from echo-sounder measurements. In a comparison of these data with the determined depth co-ordinates from the ISSS system, accuracies from about 0.6 to 0.8 m were found. This is not as exact as echo-sounding, but seems adequate for many applications. Future hardware developments can increase accuracy and reduce the weight of the tow-fish to get an operational topographic sonar system.

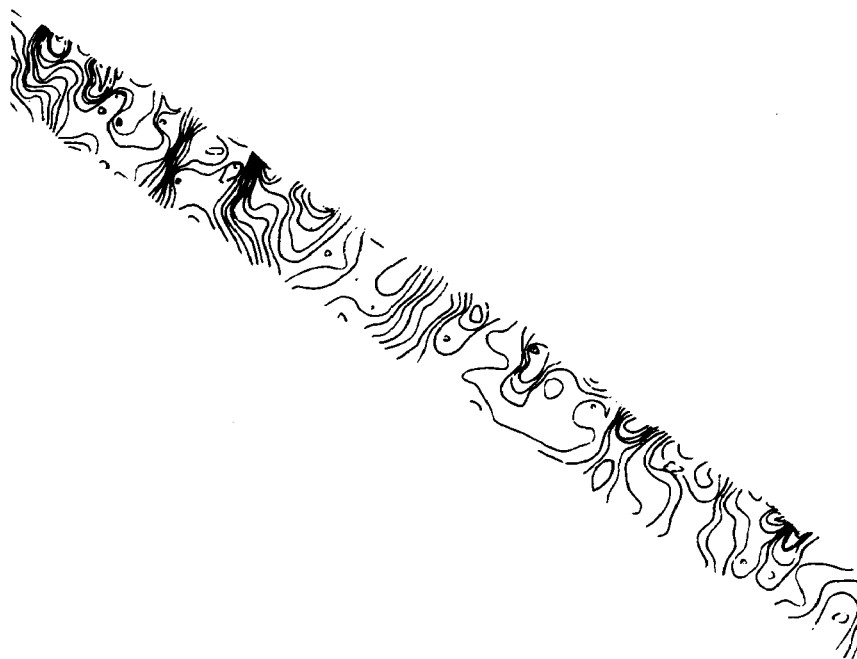


FIG. 14. — Automatic processed sea map (plotting with TASH, KRUSE, 1980).

REFERENCES

- BELDERSON, R. (1972) : Sonographs of the sea floor. A picture atlas. Elsevier Publishing, New York.
- CASTLEMAN, K. (1974) : Digital image processing. Prentice Hall.
- CHESTERMAN, W.D., ST. QUINTON, J.M.P., CHAN, Y. & MATTHEWS, H.R. (1967) : Acoustic surveys of the sea floor near Hong Kong. *Intern. Hydrogr. Review*, Vol. XLIV (1), January.
- CLERICI, E. (1977) : Über die Anwendbarkeit von Side Scan Sonar zur Erstellung von topographischen Karten des Meeresbodens. Wissenschaftliche Arbeiten der Fachrichtung Vermessungswesen der Universität Hannover Nr.71, Dissertation.
- DENNERT-MÖLLER, E., EHLERS, M., KOLOUCH, D. & LOHMANN, P. (1982) : Das digitale Bildverarbeitungssystem MOBI-DIVAH. *Bildmessung und Luftbildwesen* Nr. 50, Heft 6.
- EHLERS, M., KOLOUCH, D. (1982) : Interferometrisches Sonar, Datengewinnung und digitale Filterung. *Bildmessung und Luftbildwesen*, No. 50.
- HEATON, M.J.P. & HASLETT, R.W.G. (1971) : Interpretation of Lloyd mirror in side-scan sonar. Seminar on Side-scan Sonar Application, University of Bath.
- KLEPSVIK, J.O. (1983) : Statistical characteristics of the sea-bed with applications to wide swathe bathymetric mapping. Institut for Almen Fysikk, Universitetet Trondheim, Dissertation.
- KOLOUCH, D. (1980) : Erstellung topographischer Karten aus interferometrischen Aufnahmen aktiver Sensoren. Internationaler Kongress für Photogrammetrie, *Internationales Archiv für Photogrammetrie*, Band XXIII, Hamburg.
- KOLOUCH, D., DENNERT-MÖLLER, E., LOHMANN, P., EHLERS, M., BÄHR, H.P. (1981) : Digitale Verarbeitung von Fernerkundungsaufnahmen. *Zeitschrift für Vermessungswesen*, Nr. 106, Heft 3.
- KOLOUCH, D. (1983) : Geometrische Auswertung von Sonarbilddaten und Interferometeraufnahmen mit Hilfe digitaler Bildverarbeitung. Wissenschaftliche Arbeiten der Fachrichtung Vermessungswesen der Universität Hannover, Nr. 124, Dissertation.
- KOLOUCH, D. (1983) : Interferometrisches seitwärts schauendes Sonar. Ein System zur flächenhaften topographischen Seevermessung. *Zeitschrift für Vermessungswesen*, Nr. 108, Heft 11.
- KRUSE, I. (1980) : TASH, Topographisches Aufnahme- und Auswertesystem der Universität Hannover. Seminar "Wattvermessung", Institut für Kartographie, Hannover.
- MITTLEMAN, J.R., MALLOY, R.J. : Stereo side-scan sonar imagery. Naval Civil Engineering Laboratory.
- PARKER VERBOOM, F.S. (1982) : Interferentie sonar, overzicht van de ontwikkeling van een interferentie sonarsystem. Rijkswaterstaat, Meetkundige Dienst, Delft.
- SFB 149 (1980) : Jahresbericht 1979, Wissenschaftliche Arbeiten der Fachrichtung Vermessungswesen der Universität Hannover, Nr. 96.
- SFB 149 (1983) : Jahresbericht 1982, Wissenschaftliche Arbeiten der Fachrichtung Vermessungswesen der Universität Hannover, Nr. 125.
- STUBBS, A.R., MCCARTNEY, B.S. & LEGG, J.G. (1974) : Telesounding, a method of wide swathe depth measurement, *Intern. Hydrogr. Review*, LI (1), January.